Internship report

Tuning cement hydration using ultrasound

Martin Chaigne

May 2019 – July 2019

Abstract

The use of ultrasound in the cement industry is the object of a new-found interest, even though research on the topic remains in its very early stages. Ultrasonication could indeed be used in order to spread effectively supplementary material within cement paste, thus improving its mechanical properties and durability and reducing its carbon footprint. However, the effect of ultrasound on the long-term mechanical properties of hardened cement paste alone have never been studied so far. This is what the following report focuses on. The mechanical properties of samples sonicated with varying duration and ultrasonic amplitude were assessed with the microindentation, microscratch and nanoindentation techniques. Results demonstrate a clear deterioration of cement paste's plastic and elastic properties due to sonication; as well as a modification of the fracture behavior.

Acknowledgements

In the first place, I would like to thank my two supervisors, Thibaut and Sébastien, for their continued support, their caring and their valuable advice. I have learned a lot from them. I would also like to thank Sama, who helped me, among other things, with the SEM imaging; and Traian, who showed me how to prepare cement samples. Finally, I would like to thank all the other members of the group and the other interns, who contributed to making these three months such a great and rich experience.

Contents

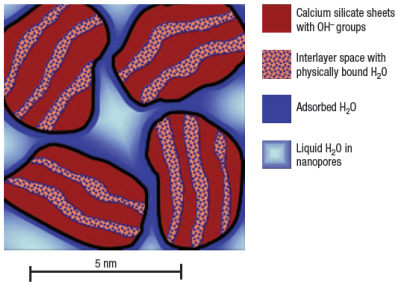

(a) Schematic representation of a C-S-H colloid [2].

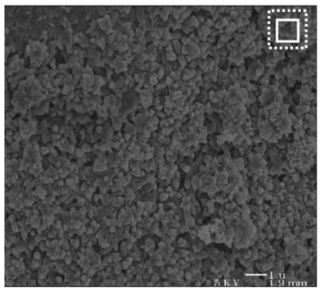

(b) SEM picture of cement paste at 10^{-6} m [4].

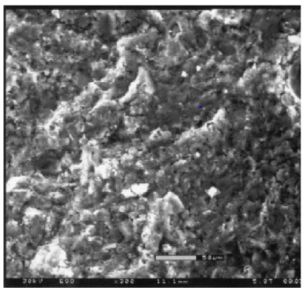

(c) SEM picture of cement paste at 10^{-4} m [4].

Figure 1: Structure of cement paste at different length scales.

1 Introduction and context

With one cubic meter produced per year and per capita, concrete is the most used building material in the world. Yet the manufacturing of cement, its main component, is very energy intensive: it accounts for more than 5% of the total anthropogenic CO_2 emissions. Finding new way of tuning cement's structure in order to enhance its mechanical properties and durability is therefore of prime importance. Whether directely or as a tool to incorporate and spread other materials, the use of power ultrasound for this purpose has recently been considered an avenue worth exploring [1]. But further discussion on how that could work requires some basic knowledge on both cement paste and ultrasound.

1.1 Cement paste

Cement paste results from the admixture of water with clinker, a powder mainly composed of calcium silicates. The dissolution of the reactive species contained in the clinker is followed by several chemical reactions. The main product of this hydration process is called C-S-H (Calcium-Silicate-Hydrate). C-S-H comes in the form of colloids, each composed of a few layers of calcium silicates separated by water molecules and calcium ions. Their typical size is 5 nm. A schematic of a C-S-H colloid is shown figure 1a [2].

Theory, confirmed by direct force measurements, indicates that the effective interaction between these C-S-H colloids is the sum of a short-range attraction and a long-range electrostatic repulsion. It results in the existence of a potential well and a shoulder, whose height is controlled by the ionic concentration of the paste. At the beginning of hydration, the low concentration in ionic species leads to a high shoulder which cannot be overcome. But as the different reactions go on, different ions are released, thus increasing the ionic concentration and reducing the height of the shoulder. It eventually allows the C-S-H colloids to aggregate and form a stress-bearing network, which densifies as hydration products precipitate within its pores [3]. This is how hardened cement paste is formed after a few hours, even though reactions continue to occur during several weeks.

The solid paste theerby obtained is a particularly complex material. It exhibits heterogeneities at different length scales and a multiscale network of pores, as can be seen on

the SEM (scanning electron microscopy) images obtained by Constantinides *et al.* and presented on the two pictures 1b and 1c [4]. It is amorphous and out-of-equilibrium. Consequently, the structure of the hardened cement paste depends on the history of the gelation and on the properties of the soft, early C-S-H gel [5].

1.2 Ultrasonication

Even though the typical wavelength of ultrasound is of a few centimeters, sonication has indeed the ability to induce mass and heat transfers at much smaller lengthscales. This is due to an effect called cavitation: the growth and collapse of microbubble in a liquid. As a matter of fact, ultrasound is an acoustic wave whose propagation is due to the alternation of compression and rarefaction in the traversed medium. If the negative pressure caused by rarefaction is strong enough, a cavity might form. It is rapidly filled with vapor coming from the surrounding medium. Under some conditions, the cavity can grow and survive several compression-rarefaction cycles, but it eventually collapses. At that time, a shock wave is emitted, and there are, locally, extreme conditions of temperature and pressure. Jets of liquid are projected at high speed. Colloids present in the liquid may collide, aggregates may deagglomerate.
It is therefore no surprise that ultrasonication has a large range of applications, such as enhancement of chemical reactivity, surface cleaning or homogenization of colloidal solutions.

1.3 Ultrasonication of cement paste: state of the art

Ultrasound at low power have often been used to investigate, in a non-invasive way, the mechanical properties of cement. Yet to the best of our knowledge, only one study has been realized on the influence of ultrasound at high power on cement paste. It is a thesis by Simone Peters (Bauhaus-Universität Weimar) defended in 2016 [6]. It focuses on the initial strength developmnent of sonicated cement paste, and is thus a kinetic study. One of the methods used by the author to follow the kinetics of hydration is isothermal calorimetry. Indeed, the chemical reactions occuring within cement paste are exothermic: measuring its heat release therefore gives some insight to the hydration process. Results are shown figure 2a. Compared to the reference sample, the peak in the heat release rate appears earlier for cement paste which has been treated with ultrasound, and reaches a higher value. The author also took SEM images of a diluted cement suspension, at the scale of the micrometer. Those which can be observed on figure 2b were taken after 5h30 of hydration. While the first C-S-H phases barely appear in the reference sample, they are much bigger in the sonicated one. It indicates that the process of precipitation and growth is more advanced in the second case.
These two results, supported by other measurements (notably conductimetry or p-wave velocity) lead to one simple conclusion: ultrasonication accelerates hydration. In order to explain this observation, Peters proposes that shock waves induced by ultrasonication remove the C-S-H precipitates from the clinker grains. These C-S-H precipitates then act as additionnal nucleation sites, and the unhydrated clinker grains remain directly in contact with water, thus enhancing hydration.

Since this research is the first one to deal with the influence of ultrasound on the

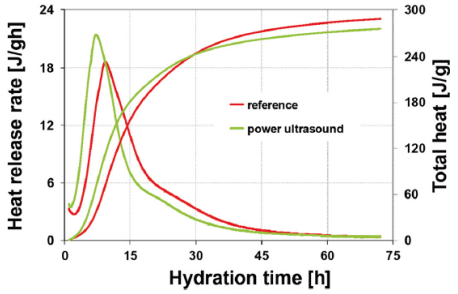

(a) Heat release rate and total heat release of cement paste during the first hours of hydration, whether it has been sonicated or not.

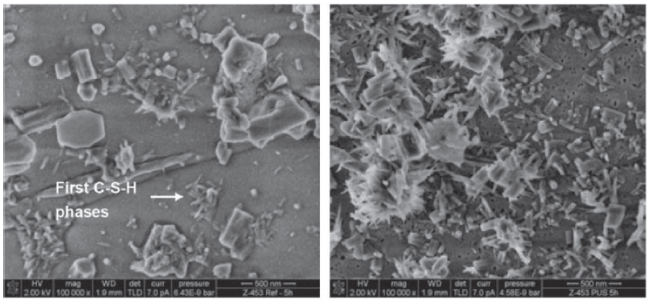

(b) SEM images of a cement suspension after 5h30 of hydration. The first C-S-H phases appear in the reference suspension (left) while they are already well-developed in the sonicated suspension (right).

Figure 2: Heat release curve and SEM images evidencing an acceleration of hydration due to sonication (Peters, 2016).

hydration of cement paste, a lot remains to be done. That's why a recent review by Ganjian *et al.* on the application of ultrasound to cementitious materials calls for more investigation on the topic [1]. One of the authors' hopes is notably to use sonication in order to disperse supplementary cementitious materials, such as silica fume, within cement paste. Adding silica fume in cement paste has indeed been known to enhance the mechanical properties of the hardened paste. But silica fume nanoparticles tend to aggregate, which significantly reduces their effectiveness. This problem could be solved by sonicating the mixture. However, sonication could also affect cement itself, and Peters' thesis suggests that it does. Hence the necessity, before even beginning to discuss the industrial feasibility of the process, to answer this simple question: does ultrasonication, while cement paste is still liquid, affect the mechanical properties of the hardened paste at long times? This was the purpose of my internship, and is the object of the rest of the report.

2 Experiments and methods

In this section, I will first describe how the set of samples was prepared, and then I will describe and explain the methods that were implemented in order to caracterize the mechanical properties of the samples.

2.1 Preparation of the samples

All the samples tested in this research were initially prepared by mixing, during 3 min, 70 g of Ordinary Porland Cement clinker powder with 42 g of water. It produced a liquid paste defined by a water-to-cement ratio of 0.6. This liquid paste was then placed in a metallic beaker and sonicated with a high intensity ultrasonic processor (*Sonics Vibra-Cell*), whose picture is presented figure 3a. It is composed of a piezoelectric transducer, which converts electrical signal to mechanical vibrations, and a probe which amplifies the vibrations. The probe tip was plunged in the liquid paste, thus creating in it ultrasound

(a) Ultrasonic processor.

(b) Demolded cylinder of hardened cement paste.

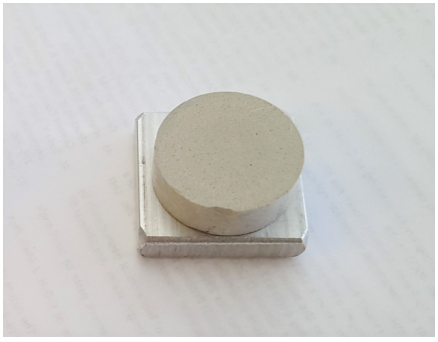

(c) Polished slice of hardened paste.

Figure 3: Experimental protocol: different steps of the preparation of the samples.

at a fixed frequency of 20 kHz.

Two main parameters of control were modified to form the different samples: the sonication duration and the amplitude of the probe. A first series of samples was prepared with sonication duration ranging from 1 to 6 minutes. Sonication was performed on the one hand continuously, and on the other as a series of pulses of 1 s interrupted by pauses of 1 s. As cavitation induced a non negligible heating of the cement paste, experiments with a sonication duration longer than 2 min were realised with and without ice bath. A second series of samples was prepared at fixed sonication duration (3 min) with different amplitudes of the probe tip, from 0 to 114 µm.

Right after the sonication process, cement paste was cast in cylindrical molds (diameter 1.3 cm and length 7 cm) and cured in a calcium hydroxide bath at room temperature during 9 days. After 9 days, cylinders of hardened cement paste, as the one presented figure 3b, were removed from their molds and kept in sealed plastic bags. After 28 days, slices approximately 1 cm thick were cut from the cylinders with a diamond saw. One face was then polished by hand with abrasive papers (*CarbiMet*, Buehler) of decreasing roughness, until the surface became reflective. Such a slice is shown figure 3c. The aim was for the two sides of the slices to be parallel and for the roughness of the polished face to be below 1 µm. It was crucial to ensure the reliability of the indentation and scratch tests which were performed afterwards, and which I will know explain.

2.2 Caracterization of the samples

The different samples were caracterized after 28 days with two complementary methods: indentation gave access to the plastic and elastic properties of the material, while scratch gave access to its fracture properties.

2.2.1 Indentation

The indentation technique, as its name indicates, consists in indenting a material with a diamond tip. A schematic of an indentation test is shown figure 4a. The normal force applied by the tip on the sample is controlled, and the indentation depth is measured. The process can be divided into three steps, separated by black dashed lines on figure 4b. During the first step, called loading, the applied normal force is increased linearly with time. As a result, the tip sinks in the material, which undergoes plastic and elastic deformation. Then in a second step, the applied force is kept constant. Contrary to a perfectly elastic material, cement paste deforms under these conditions: it *creeps*. This behavior is due to the rearrangement of cement colloids near the surface of contact. Finally, in a third step called unloading, the applied force decreases until contact between the tip and the sample ends. In the meanwhile, the material undergoes a purely elastic recovery.

Hardness and indentation modulus A method described by Oliver and Pharr [7] is used to calculate the hardness H and the indentation modulus M from the data obtained during an indentation test. Hardness refers to the ability of a material to resist plastic deformation. The indentation modulus is an effective elastic modulus defined by:

$$\frac{1}{M} = \frac{1-\nu^2}{E} + \frac{1-\nu_i^2}{E_i}, \tag{1}$$

where E, ν, E_i and ν_i are the Young's Modulus and the Poisson's ratio of the indented material and of the indenter, respectively.
Both mechanical properties are directly deduced from the analysis of the force versus indentation depth curve, as the one plotted figure 4c. Hardness is indeed given by:

$$H = \frac{F_{max}}{A_c}, \tag{2}$$

where F_{max} is the maximal force applied during the test; and A_c, the area of contact between the indenter and the material, is a calibrated function of the maximal indentation depth h_{max}. The indentation modulus M is linked to the stiffness of the material S, which is the derivative of F with respect to h evaluated in h_{max}, according to the following equation:

$$M = \frac{1}{\beta}\frac{\sqrt{\pi}}{2}\frac{S}{A_c}, \tag{3}$$

where β is a correction factor depending on the shape of the indenter.

Creep modulus Indentation gives access to a third mechanical property of the material: the creep modulus. It describes the material's behavior under constant load. That is why the variation of the indentation depth as a function of time during the period when

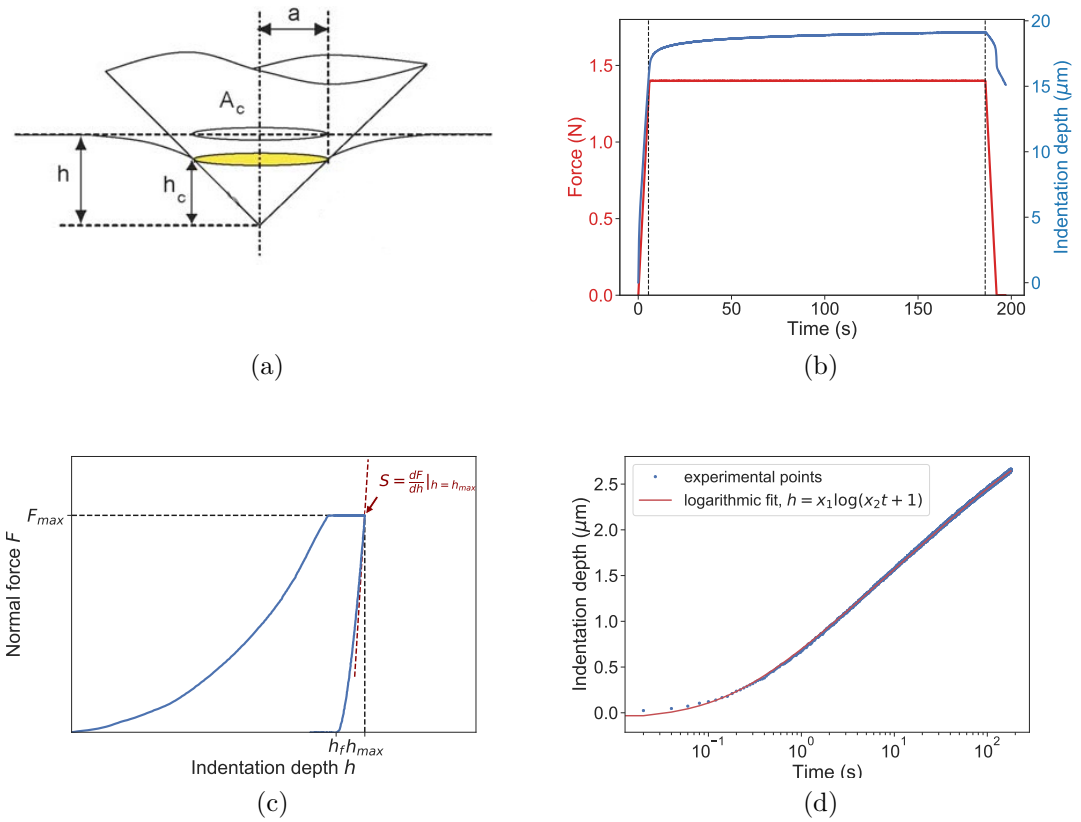

(a) (b) (c) (d)

Figure 4: Principle of the indentation test: (a) schematic of an indentation (Constantinides *et al.*, 2006); (b) variation of the applied normal force and of the indentation depth with time; (c) normal force as a function of the indentation depth; and (d) renormalized indentation depth as a function of time during the creep period (when the normal force is kept constant), with logarithmic fit.

the applied force is constant is plotted figure 4d. As Vandamme and Ulm noticed and explained [8], this curve is well-approximated by a logarithmic fit of the form $h(t) = x_1 \log(x_2 t + 1)$. The creep modulus C is obtained from the fitting parameter x_1:

$$C = \frac{F_{max}}{2\sqrt{\frac{A_c}{\pi}} x_1}. \tag{4}$$

The indented material creeps all the more that its creep modulus is low.

Choice of the indentation depth The indentation depth must be carefully chosen, because it has huge implications on the results. Cement paste indeed exhibits heterogeneity at different length scales. At the scale of a few micrometers, cement paste is composed of different phases differing by their chemical composition (unhydrated clinker, C-S-H or other hydration products) or their packing density. At a much larger scale, cement paste appears as homogeneous.

When an indentation is performed at a given depth h, it probes the mechanical properties of a volume of material whose characteristic size is comprised between 3 and $5 \times h$.

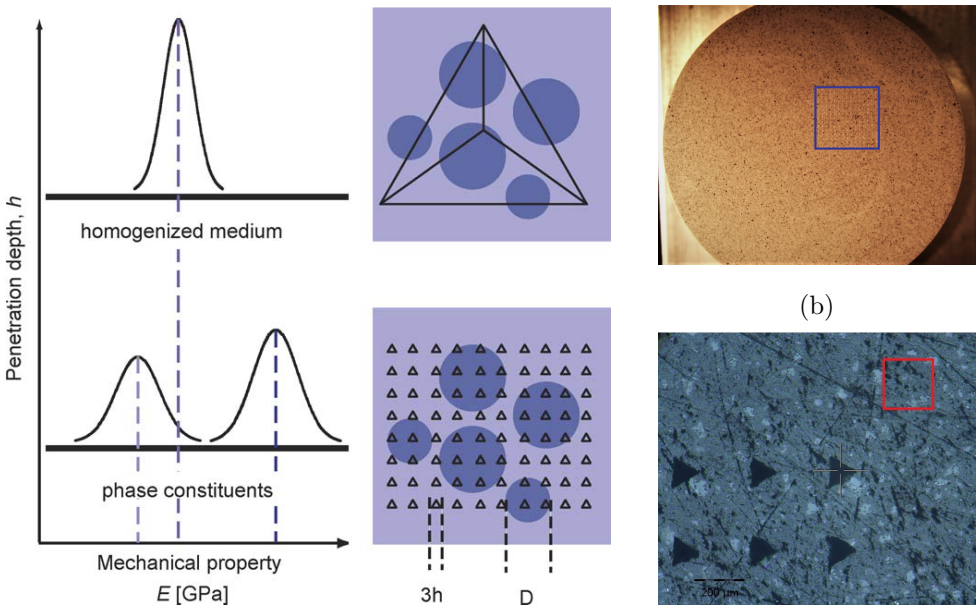

Figure 5: 5a Schematic illustrating the difference between microindentation and nanoindentation (Constantinides *et al.*, 2006); 5b photograph of a polished sample on which a microindentation grid was performed; the grid (surrounded by a blue square) is composed of 15×15 indents of depth 18 µm separated by 300 µm; and 5c image of the same sample obtained by optical microscopy; some indents from the microindentation grid appear on the bottom left part; the red square identifies the location of the nanoindentation grid, which is composed of 21×21 indents of around 200 nm depth separated by 10 µm.

Consequently, if the indentation depth is greater than a few micrometers, an indentation test will give access to the mechanical properties of the composite material. Repeating the test several times will lead to values following a Gaussian distribution, as explained by the upper part of the schematic 5a. On the contrary, if the indentation depth is much smaller than one micrometer, one indentation will give access to the mechanical properties of one specific phase. By repeating the test several times, one will probe the properties of the different phases: the values of hardness, indentation modulus and creep modulus will therefore be distributed as a set of Gaussian curves, as suggested by the lower part of the schematic 5a.

These two different tests were performed on the samples. Indentation at a depth larger than the micrometer, typically $18 - 20$ µm, will now be referred to as microindentation. In order to have a statistically significant set of data, 225 microindents were done on each sample. They were organized as a grid of 15×15 indents separated by 300 µm, as shown on the picture 5b.
Indentation at a depth shallower than the micrometer, typically $200 - 300$ µm, will now be referred to as nanoindentation. As nanoindentation probes different phases and not only one composite medium, the number of indents required to have a significant set of data is even higher: 441 indents were done on the analyzed samples. They were organized as a grid of 21×21 indents separated by 10 µm. The picture 5c, obtained with an optical microscope with 20× magnification, shows the location of a nanoindentation grid

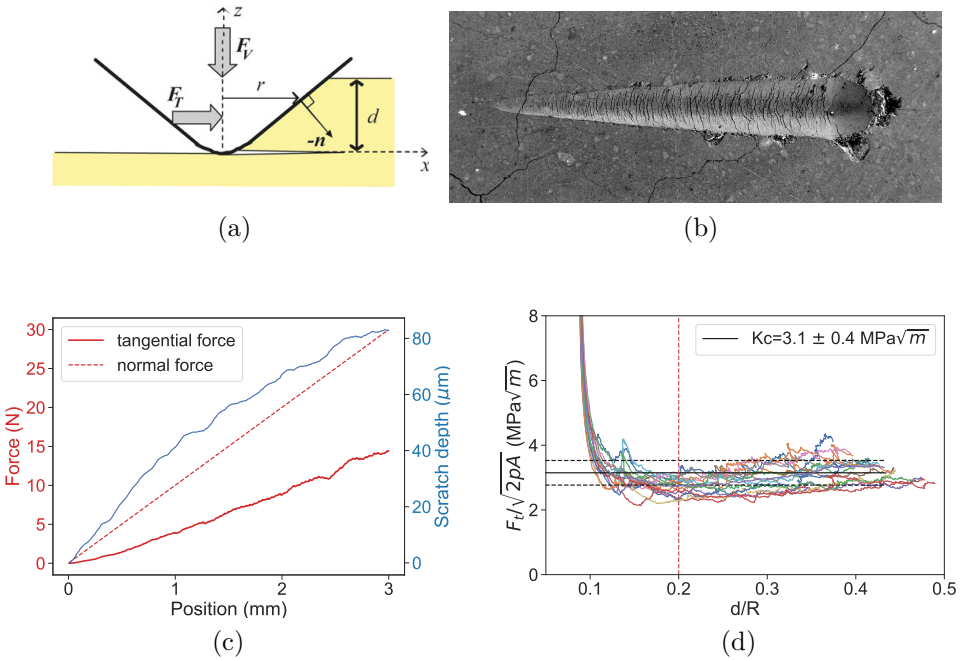

Figure 6: (a) schematic of a tip performing a scratch (Akono *et al.*, 2011); (b) SEM picture of a 3 mm scratch performed on the reference sample; (c) variation of the prescribed normal force and of the measured tangential force and depth of the tip during a scratch test; and (d) plots showing the row data for the 15 scratches performed on the reference sample, and a clear convergence to a constant value of the fracture toughness K_c.

(surrounded by a red square) on a sample which had previously been microindented.

2.2.2 Scratch

A second method was used to characterize the samples, and more specifically their fracture properties: scratch.
The principle of such a test is illustrated figure 6a. A conical tip is moved laterally on the sample of interest while the prescribed normal force is linearly increased. The process is rapidly driven by fracture. On the SEM picture 6b of one scratch of length 3 mm (performed on the reference sample), one can indeed notice the numerous cracks in the direction perpendicular to the scratch. During one scratch test, two quantities are measured: the tangential force F_t exerted horizontally by the material on the tip, and the depth of the tip d. A typical plot featuring these quantities (obtained from a scratch on the reference sample) as well as the prescribed normal force is shown figure 6c.

In two seminal papers published in 2011, Akono *et al.* demonstrate that data obtained during a scratch test allow to determine the fracture toughness of a given material [9] [10] . The fracture toughness K_c is a mechanical property, expressed in MPa$\sqrt{\text{m}}$, which depicts the ability of a material to resist fracture. Thanks to dimensional analysis and energetic considerations, the authors show the following relationship between K_c and the quantities

measured during a scratch:

$$K_c = \frac{F_t}{\sqrt{2p(d)A(d)}}, \tag{5}$$

where $p(d)$, the probe perimeter, and $A(d)$, the load-bearing projected contact area between the probe and the material, are functions of the depth d only. The explicit expressions of p and A as a function of d are calibrated for a given probe geometry (in our case, a Rockwell conical probe with a spherical extremity of radius $R = 200$ µm).
Kabir *et al.* later showed that, provided the tip displacement speed is high enough, the fracture toughness measured in doing so is independent of the speed at which scratch is performed [11].

Figure 6d shows the variation of $F_t/\sqrt{2pA}$ as a function of the ratio d/R, R being the radius of the spherical extremity of the tip, for 15 scratches realized on the reference sample. For small values of d/R, when the scratch process is not dominated by fracture and by the conical shape of the tip, $F_t/\sqrt{2pA}$ diverges. However , for larger values of d/R, it rapidly tends to a constant, as predicted by equation 5. This constant is the fracture toughness. K_c is therefore computed as the mean value of $F_t/\sqrt{2pA}$ above a certain threshold (here $d/R = 0.2$, indicated by a red dashed line), averaged on the 15 scratches performed on the sample.

3 Results and discussion

In this section, results evidencing an influence of ultrasonication on the macroscopic mechanical properties of cement paste will be presented. These results were obtained with the two distinct techniques described above: microindentation and scratch. Then, a discussion on how to explain the changes observed at the macroscopic scale on sonicated samples will be engaged. It will be based, in particular, on nanoindentation and SEM results.

3.1 Influence of ultrasonication on the plastic and elastic properties of cement paste

First, we will see how ultrasonication of the liquid cement paste affects the plastic and elastic properties of the hardened paste, more specifically hardness, indentation modulus and creep modulus. These properties were investigated with the microindentation technique described in the previous section. A Micro Indenter from Anton Paar was used, with a Berkovich tip.

3.1.1 Influence of ultrasonication duration

The first series of samples that will be considered is the one for which ultrasonication was realized at fixed amplitude but with varying duration.
Figure 7 gives a comprehensive account of the data gathered on four particular samples: the reference sample on which no ultrasound was sent, and samples which were continuously sonicated during respectively one, two and four minutes. On the left, figure 7a, data is presented as a plot of the indentation modulus M as a function of the hardness. Each

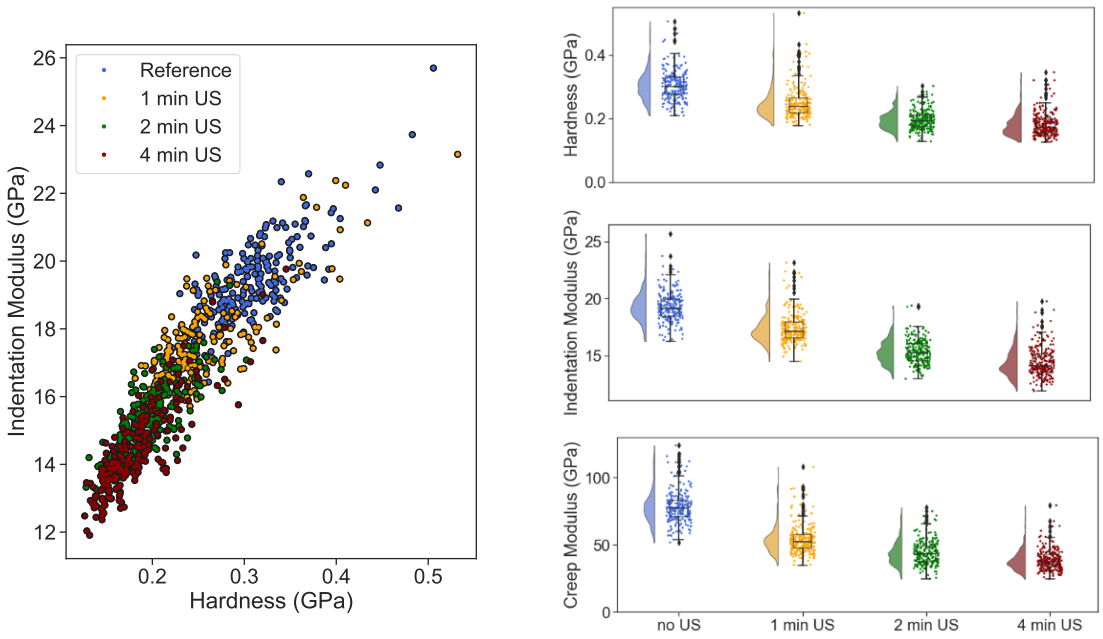

(a) (b)

Figure 7: (a) Indentation modulus *versus* hardness for all indentations performed on four different samples, the reference and samples continuously sonicated during 1, 2 and 4 min; (b) *raincloud* plots of the three mechanical properties deduced from microindentation for the 4 same samples; they give in each case a comprehensive idea of the raw data, its distribution, range, median, first and third quartiles.

point corresponds to one of the 225 indentations that were done on each sample. The color of a point indicates on which sample the indent was carried out. It can be noted that all the points seem to be distributed along the same line. This is an interesting information, since the hardness-indentation modulus is almost a signature of a material. The plot therefore suggests that sonication does not induce any significant change in the final hardened paste's chemical composition.

However, even if they are distributed along the same line, the point clouds belonging to each of the four samples do not overlap. The longer ultrasound was applied in a sample, the more the corresponding point cloud is shifted toward low values of hardness and indentation modulus.
This observation is confirmed by the *RainCloud* plots presented figure 7b. They give, for each mechanical property and each sample, a good vision of the data obtained: its statistical distribution, its range, its median value and first and third quartiles. It appears very clearly that sonication induces a weakening of cement paste: hardness, indentation modulus as well as creep modulus all significantly decrease when the sonication duration increases. The drop is even more dramatic for the two plastic properties, hardness and creep modulus. Hardness indeed decreases from 0.30 ± 0.05 GPa (mean value $\pm$ standard deviation) for the reference sample to 0.18 ± 0.04 GPa for the sample sonicated during 4 minutes, that is, a drop of 40%. Creep modulus likewise decreases from 78 ± 12 GPa (mean value $\pm$ standard deviation) to 39 ± 8 GPa, which is a drop of 50%. Indentation

modulus, for its part, experiences a decrease of 26% (from 19 ± 2 GPa to 14 ± 2 GPa); which, even if less spectacular, remains far from being negligible.

It has thus been observed that ultrasonication of an early liquid cement paste during a few minutes causes a clear weakening of the hardened cement paste 28 days later. This effect is apparently not due to a change in the chemical composition of the cement paste; it is probably a texture effect.

However, the origin of such an effect remains unclear. Temperature of the cement paste was recorded during the sonication process. It was noticed that sonication induced a significant heating of the paste: from 23 °C to 46 °C after 1 min and 65 °C after 4 min. A natural question then arises: is the observed deterioration of the mechanical properties only due to the typical cavitational effects (shock waves, particle collisions...), or also, at least partly, to the cavitation-induced heating? Next part aims to answer it.

3.1.2 Influence of sonication-induced heating

Since sonication induced a heating of the paste, it was decided to redo in an ice bath all samples whose temperature had risen above 55 °C, which means all samples sonicated during more than 2 min. 60 °C is indeed known to be a threshold above which new reactions can occur in the paste. The ice bath effectively reduced the heating : the sample sonicated during 4 min only reached 46 °C, as opposed to 65 °C without ice bath.

Figure 8 shows the mean values and standard deviations for H, M and C, for samples sonicated both with and without ice bath, and therefore allows a comparison. Data corresponding to samples continuously sonicated without ice bath are indicated by red markers. These are the same data than those shown in a different form on the raincloud plots 8. Data corresponding to samples continuously sonicated within an ice bath are indicated by blue markers.
In almost all cases, data obtained with or without ice bath overlap if errorbars are taken into consideration. It tends to prove that the effect we observed is not an effect of temperature, but an actual effect of ultrasound.

Moreover, figure 8 also shows the microindentation results for the samples which were sonicated by a series of 1 s pulses and 1 s pauses, instead of continuously. The sonication duration considered here is the total duration during which ultrasound was effectively sent. The data do not show any significant deviation from the continuous sonication case. It can be concluded that the relevant parameter is the sonication duration, and it doesn't matter whether sonication was continuous or not.

The results discussed so far, concerning samples treated with ultrasound at fixed amplitude but varying duration, show that sonication deteriorates the hardness, the indentation modulus and the creep modulus of the cement paste. The longer sonication lasts, the weaker the hardened paste becomes. However, it seems that a plateau is reached: between 3 and 6 minutes of sonication, there does not seem to be a clear decrease in the values of H, M and C.
Now as a second step, the influence of the ultrasonic amplitude will be investigated.

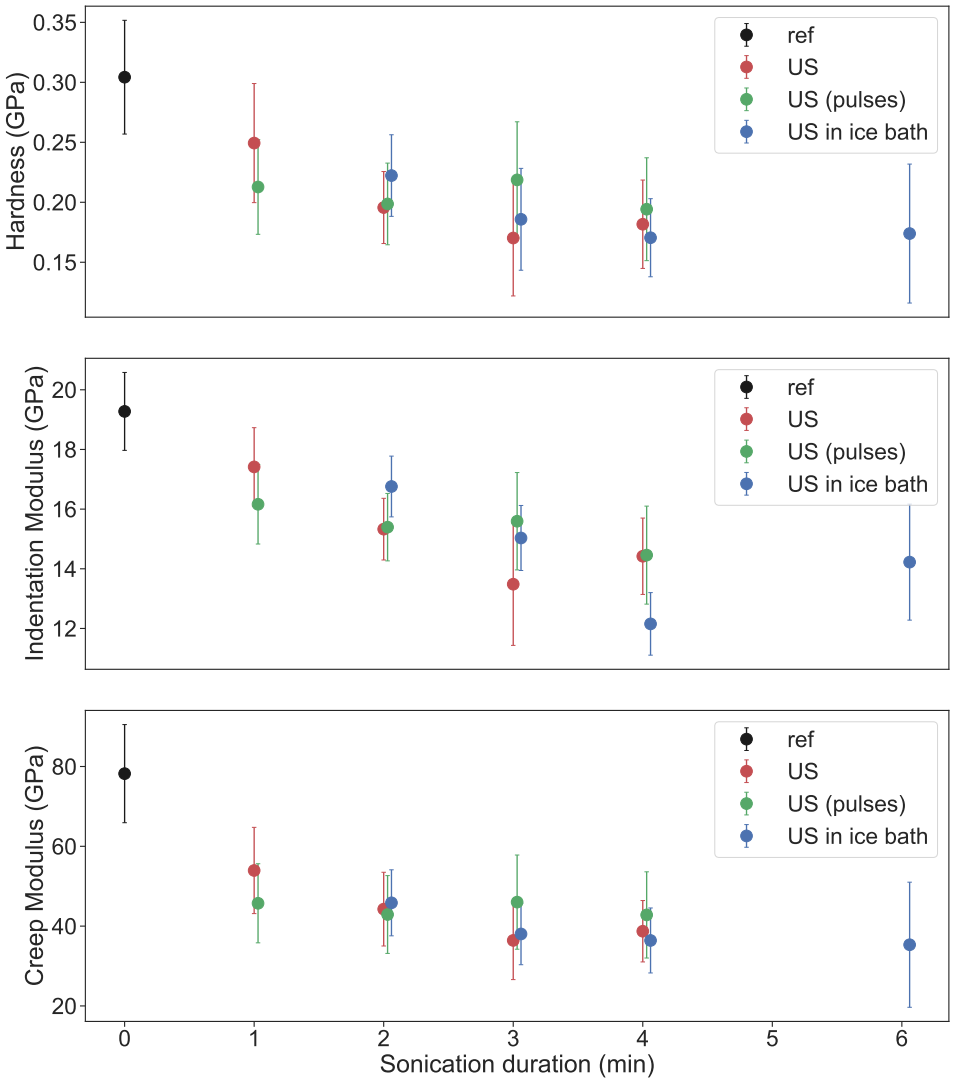

Figure 8: Variation of hardness, indentation modulus and creep modulus measured by microindentation (dots are the mean values, errorbars are the standard deviations) as a function of the sonication duration. Red markers correspond to the samples which were continuously sonicated. Blue markers correspond to samples continuously sonicated in an ice bath. Green markers correspond to samples sonicated with a series of pulses and pauses.

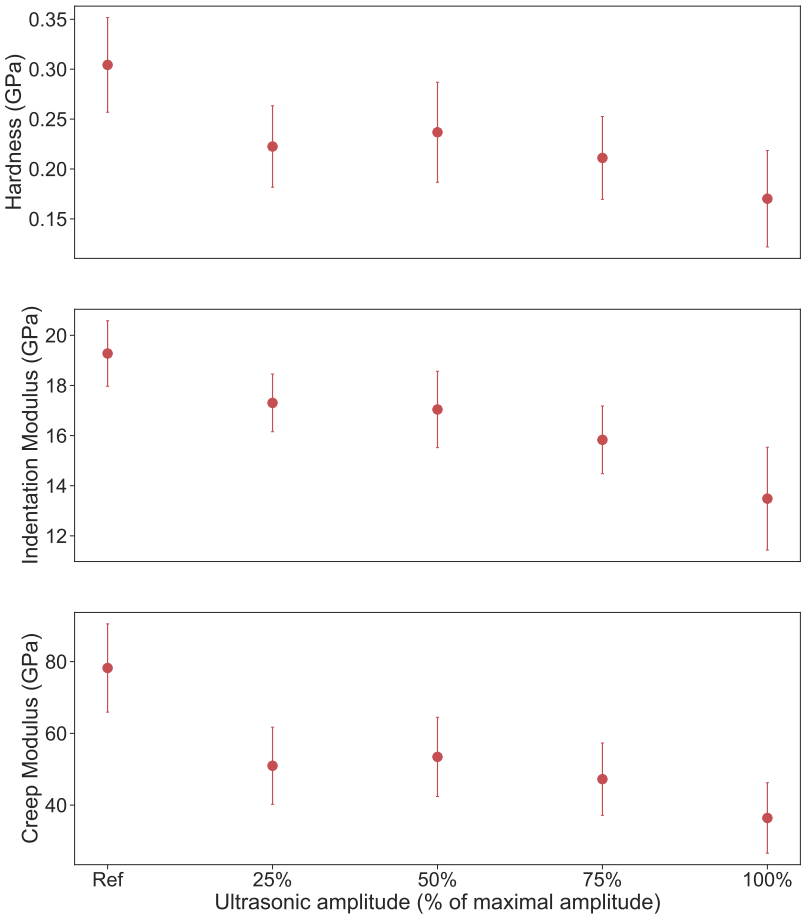

Figure 9: Variation of hardness, indentation modulus and creep modulus measured by microindentation (dots are the mean values, errorbars are the standard deviations) as a function of the ultrasonic amplitude. All samples were sonicated during 3 min.

3.1.3 Influence of the ultrasonic amplitude

The samples whose mechanical properties will be discussed here were prepared at fixed sonication duration: 3 min. Yet the amplitude of the vibrations of the ultrasonic processor's probe, which induce ultrasound, was modified.

Results are shown figure 9. The ultrasonic amplitude is expressed as a percentage of the maximal amplitude, which corresponds to a vibration of the probe of amplitude 114 µm. As it could have been expected, the three mechanical properties globally decrease when the ultrasonic amplitude increases. There is no threshold effect observed: even a sonication at 25% of the maximal amplitude significantly affects the material.

These results, combined with those formerly presented, draw a clear picture: sonication deteriorates the plastic and elastic property of cement paste. At fixed amplitude, the values of H, M and C decrease when the sonication duration increases. At fixed duration, they decrease when the ultrasonic amplitude increases.
In order to complete the overview of the influence of sonication on the mechanical prop-

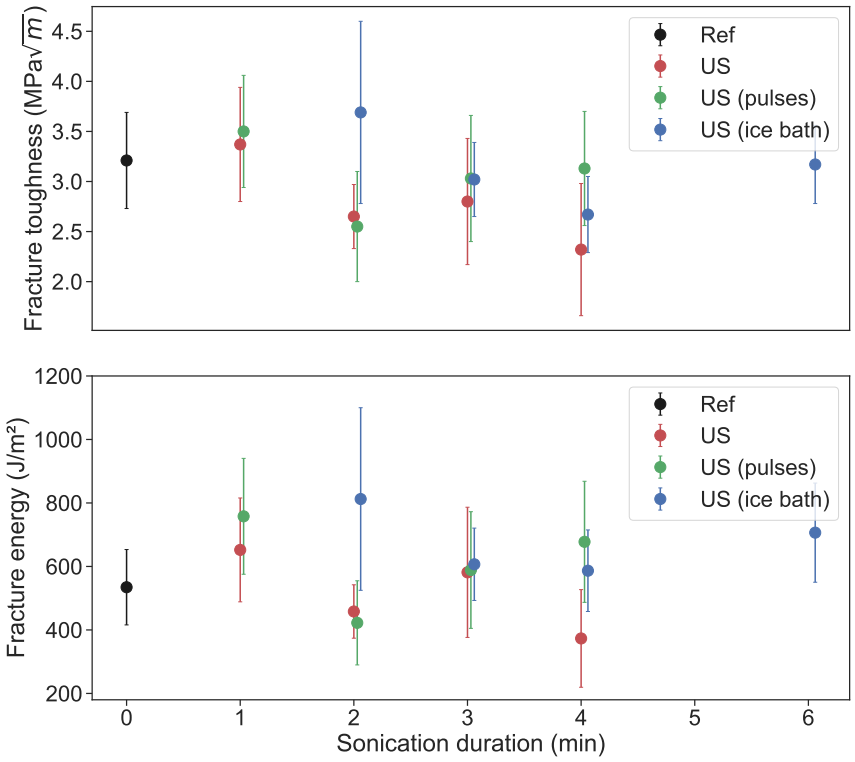

Figure 10: Variation of fracture toughness measured by scratch and of fracture energy as a function of the sonication duration. All samples were sonicated at maximal amplitude, either continuously with an ice bath (blue markers) or without (red markers), either as a series of pulses and pauses (green markers).

erties of cement paste, fracture properties also need to be investigated. It is the object of the following section.

3.2 Influence of ultrasonication on the fracture properties of cement paste

Fracture properties were studied with the scratch technique: 15 scratches were performed on each sample with a Micro Scratch Tester from Anton Paar. It measures the fracture toughness K_c of the material. Knowledge of K_c and of M (measured by microindentation) give access to the fracture energy $\mathcal{G}_c$. $\mathcal{G}_c$ corresponds to the energy per unit of area necessary to propagate a crack, and can be simply expressed as:

$$\mathcal{G}_c = \frac{K_c^2}{M}. \tag{6}$$

The values of K_c and $\mathcal{G}_c$ obtained for all samples sonicated at maximal amplitude are plotted figure 10 as a function of the sonication duration. The fracture toughness of the samples seems to be unaffected by sonication: it remains merely constant as a function of the sonication duration, around 3 MPa$\sqrt{\text{m}}$.
Even if a decrease of M with sonication duration was observed, it is unclear that the fracture energy (which is proportional to $1/M$) increases when ultrasound is applied longer.

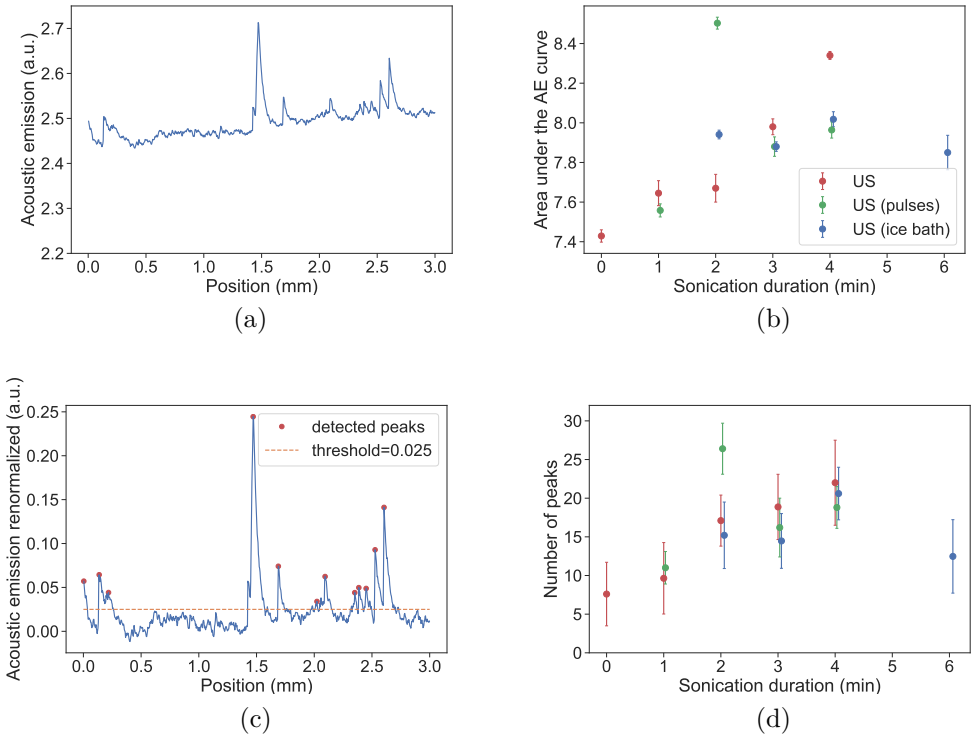

Figure 11: (a) Acoustic enegy, in arbitrary units, as a function of the position of the probe along the scratch; (b) area under the curve of the acoustic energy as a function of the sonication duration; (c) acoustic energy renormalized, arbitrary threshold and peaks detected above this threshold; and (d) number of peaks above an arbitrary threshold of 0.025 (a.u.) as a function of the sonication duration.

The errorbars being taken into consideration, it rather appears that $\mathcal{G}_c$ remains constant, around 600 J/m^2.

These results tend to prove that sonication has little effect on the fracture properties of cement paste. However, another quantity was measured during the scratch tests: the acoustic emission. It is related to the formation of cracks (as those which could be observed on the SEM picture 6b). Analysis of the acoustic emission data therefore gives new insight into the fracture processes at stake.

Figure 11c shows the acoustic energy measured by the scratch tester as a function of the position of the probe along the 3 mm scratch, for a scratch performed on the reference sample. The average area under the acoustic energy curves was computed for each sample sonicated at maximal amplitude. Results are plotted figure 11c. Even if there are some surprising points (those corresponding to the sample sonicated with a series of pulses during 2 min and the one sonicated during 6 min in an ice bath), the trend is very clear: the area under the acoustic energy curve increases with the sonication duration. It probably means that the more a sample has been sonicated, the more it creates cracks when it is scratched, or the bigger theses cracks are.
Moreover, we investigated the number of peaks, in the acoustic emission signal, above

an arbitrary threshold. In order for the analysis to be relevant and reproducible, raw data was slightly modified. A linear function was subtracted to it, thus "correcting" both the offset and the general increase in the acoustic emission with respect to the scratch position (see figure 11a). Figure 11b shows the corresponding signal. Then, the number of peaks above arbitrary thresholds was counted for the different samples. Provided the chosen threshold was low enough (if not, standard deviations were bigger than the average values, preventing any conclusion to be reached), a clear trend emerged. With the arbitrary threshold fixed at 0.025 (a.u.) as represented figure 11b, the number of peaks detected is plotted figure 11d as a function of the sonication duration. It appears that the number of peaks increases with sonication duration. Similar graphs are obtained with other thresholds. These peaks can be interpreted as resulting from the creation of big cracks. Our results thus show that scratching cement which had been sonicated longer lead to the formation of bigger cracks: a hardened cement paste is all the more brittle that it has been sonicated for a long time.

Even if it was not captured by significant variations in the fracture toughness or the fracture energy, sonication still has an effect on the fracture properties of cement paste: it makes cement paste become more brittle.
This observation adds up to the previous findings that sonication deteriorates the elastic and plastic properties of the paste. It concludes our step of characterization at the macroscopic scale. The logical questions that now arises are: what difference exists in the microscopic structure of sonicated cement paste, compared to the reference paste, which explains the changes observed in the macroscopic mechanical properties? And by which processes did sonication lead to these structural changes? The last part of the report will try to answer these questions.

3.3 Microscopic investigation of sonicated cement paste

As explained in the "experiment and methods" section, at the scale of the micrometer, cement paste is composed of different phases which differ by their chemical composition or by their packing density. These different phases have different elastic and plastic properties.
The mean properties of the phases and their volume fraction can be recovered by statistical nanoindentation, a method developed by Ulm *et al.* [12]. It is based on the statistical analysis of the data obtained by performing 441 indentations at a depth of about 200 µm, small enough so that each indentation probes the properties of one phase only. Data therefore consists of 441 points having each 3 coordinates: (H,M,C). The objective is to find clusters in the data. Points being in the same cluster will then be interpreted as indentation performed in the same phase. The proportion of points belonging to one cluster will be interpreted as the volume fraction of the corresponding phase in the cement paste. In order to find these clusters, we used an algorithm called Gaussian Mixture Model, implemented in Python *Sci-kit learn* package. It finds clusters with a Bayesian criterion and an expectation maximization procedure; assuming that data points follow a Gaussian distribution around the centers of the clusters which have to be discovered.

As an illustration, figure 12a shows the data points obtained by nanoindentating the sample which was continuously sonicated during 4 min. They are projected on the (H,M)

plane. The plot is very different from that obtained with microindentation (see figure 7a) and it is seems clear that nanoindentation was not done on a homogeneous material. Identifying clusters, however, is not obvious; hence the need of the GaussianMixture algorithm. Figure 12b shows the same data, with a representation of the four clusters identified by the algorithm. Ellipses are centered on the mean values of the clusters, and their edges correspond to a distance of 3 standard deviations from the center. Comparison of the properties of the phases with existing studies allows their identification.
Phases represented in navy blue and orange on the graph compose the majority of the material. These phases are made of C-S-H and only differ by their packing density. The phase with the lowest values of H, M and C (here corresponding to the blue ellipse) is referred to as "low-density C-S-H". The other one (corresponding to the orange ellipse) is referred to as "high-density C-S-H". The phase corresponding to the red ellipse is probably the clinker phase (pieces of clinker which have remained unhydrated). Finally, the phase corresponding to the green ellipse is a composite phase whose composition is not precisely known: it is probably a mixture of clinker, C-S-H and other hydration products.

These four phases were identified in all samples which were nanoindented. Figure 12c shows their volume fraction for four different samples, sonicated with a varying duration (from zero to four minutes). There are some variations in the volume fractions between the different samples, but no definite overall trend. Finally, the mean value and standard deviation of the indentation modulus for each phase of the four samples are plotted figure 12d. For the sake of concision, such a graph is shown only for the indentation modulus, but hardness and creep modulus behave likewise. The plastic and elastic properties of the two C-S-H phases are similar for all samples, but they slightly decrease for the two harder phases. It may result from a reduction of the proportion of unhydrated clinker in the hardened cement paste with sonication. A simple explanation would be that clinker grains are split into pieces as an effect of sonication. Their hydration would thus be facilitated, and the fraction of clinker remaining unhydrated after 28 days would decrease.

However, it is very unlikely that this diminution of the volume fraction of clinker is enough to explain the changes observed at the macroscopic scale. And both C-S-H phases (which govern the macroscopic properties of cement) seem unaffected by sonication: neither their volume fraction nor their respective mechanical properties significantly change. Since there is no obvious structural change at the scale of the micrometer due to sonication, but a dramatic effect on the mechanical properties at the scale of hundredth of micrometers, the effect of sonication on the structure of cement paste should be at an intermediate length scale.

That's why SEM imaging was realized on a few samples sonicated with a different duration, in order to see if differences could be identified at such a scale.
Figure 13 shows SEM images of the residual impression of an indent, respectively on the reference sample (figure 13a) and on the sample sonicated continuously during 4 minutes (figure 13b). The main difference is that black inclusions of about 20 µm can be observed on the sonicated sample, on the bottom left corner and on the top right corner. Such inclusions were noticed on all sonicated samples which were imaged by SEM, suggesting a link between sonication and their presence. A systematic imaging of all samples and a quantitative estimation of their number as a function of the sonication duration still have

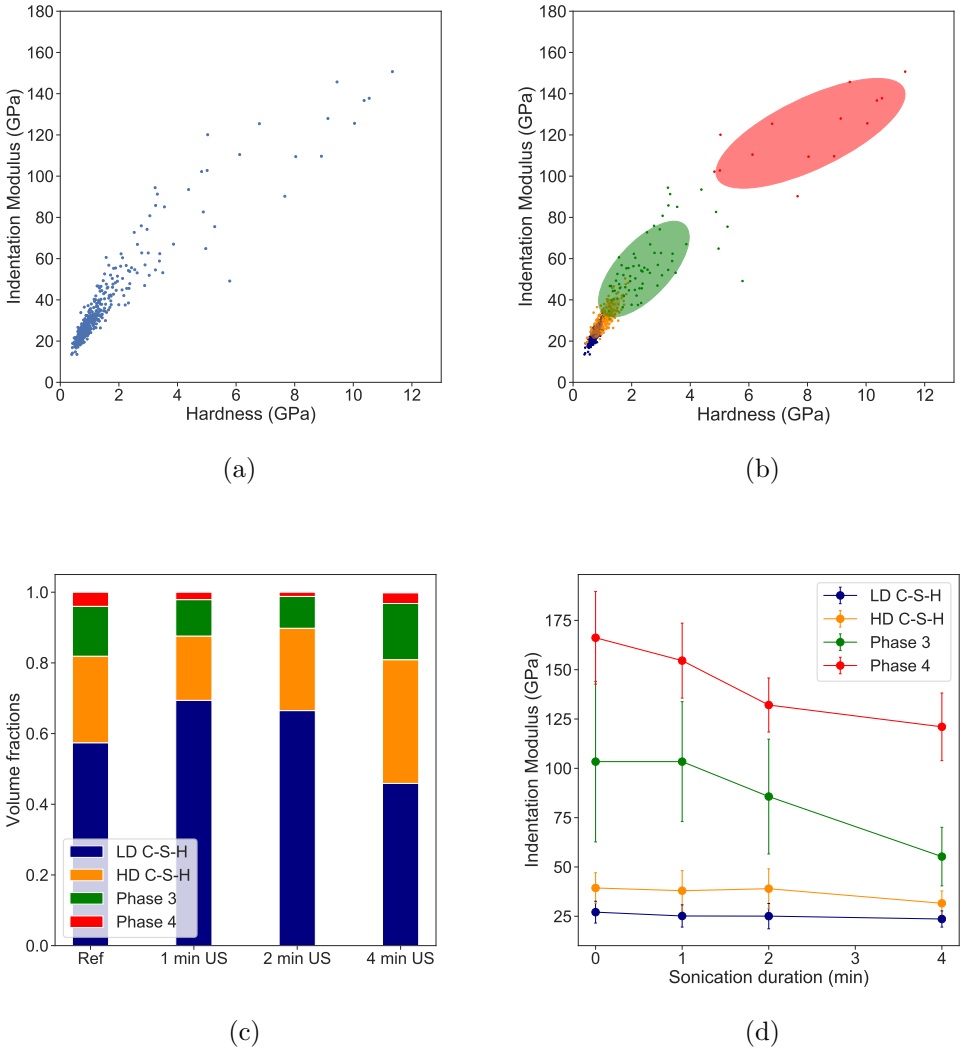

Figure 12: (a) Data points obtained with a nanoindentation grid performed on the sample continuously sonicated during 4 min, projected in the (H,M) plane; (b) same data points with ellipses corresponding to the four clusters found by the Gaussian Mixture algorithm; (c) volume fraction of the four different phases found in cement paste for samples sonicated with different duration; and (d) mean value and standard deviation of the indentation modulus for the different phases, for samples sonicated with different duration.

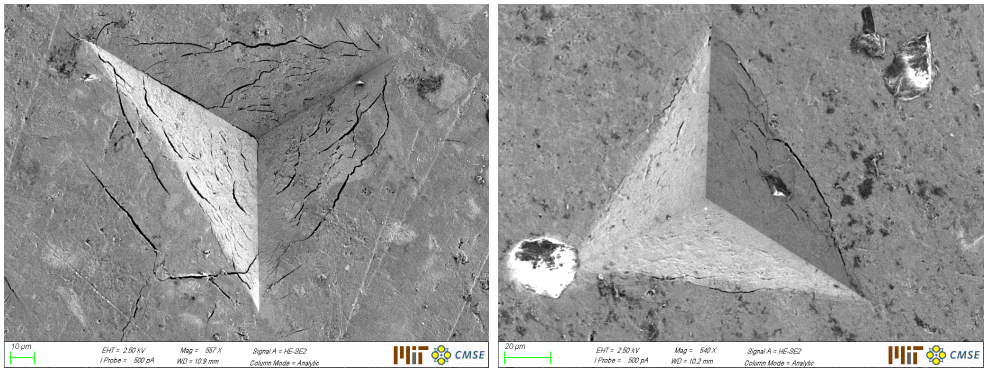

(a) (b)

Figure 13: SEM picture of the residual impression of an indent performed (a) on the reference sample and (b) on the sample sonicated during 4 min.

to be done in order to verify this hypothesis. A chemical analysis of one of these black inclusions will also be realized, and might indicate how these inclusions were created. Only afterward, the eventual influence of these inclusions in the deterioration of cement paste's mechanical properties might be discussed.

That aside, we propose a beginning of hypothesis as to the scenario leading to a sonication-induced deterioration of the mechanical properties of cement paste. In an article quoted in the introduction [5], Ioannidou *et al.* explain that in the first hours of hydration, the first C-S-H colloids precipitate and form a fibrillar network. This fibrillar network then acts as a "scaffolding" as other colloids precipitate around it in a denser way; and is therefore of prime importance in the strength development of cement. One can imagine that sonication seriously affects the establishment of this "scaffolding": perhaps sonication itself breaks into pieces the "first-draft scaffolding" which forms in the first minutes of hydration. Then the whole densification process occurs normally, but around a broken "scaffolding". It would explain both the deterioration of the mechanical properties at the macroscopic scale, and the fact that no change is observed at the microscopic scale. This hypothesis, of course, has yet to be proven.

4 Conclusion and perspectives

Different cement samples were thus prepared, sonicated with varying duration and ultrasonic amplitude while the paste was still liquid. After 28 days, the mechanical properties of the samples were tested with two techniques: microindentation and scratch.
Microindentation results show that sonication has a clear impact on the elastic and plastic properties of cement paste. At fixed amplitude, the hardness, indentation modulus and creep modulus dramatically decrease when the sonication duration increases. At fixed duration, they decrease when the ultrasonic amplitude increases.
Scratch results show that sonication also affects the fracture properties of cement paste. Even though the fracture toughness and the fracture energy are barely modified, analysis of the acoustic emission during scratch tend to prove that cement samples are all the more

brittle than they were sonicated for a long time.
In a last part, the microscopic origin of these changes observed at the macroscopic scale was investigated. It is not clear with nanoindentation results that the volume fractions and mechanical properties of the phases composing cement paste at the scale of the micrometer are modified by sonication. However, SEM microscopy revealed the presence of black inclusions in the sonicated samples. Further studies need to be implemented in order to gain knowledge about the origin of these inclusions and their link with ultrasonication.

The reasons why sonication of a liquid cement paste during a few minutes lead to such drastic differences on the hardened paste 28 days after therefore remain unclear; even though we propose a beginning of explanation.
New experiments are planned in order to have a more comprehensive overview of the issue. Samples prepared in a plastic beaker instead of a metallic one should allow to study the influence of the container; since ultrasound behave very differently when it reaches a plastic wall rather than one made of metal. Samples were also prepared without any sonication, but with an initial heating similar to that induced by cavitation in the sonicated samples. Tests performed on these samples should confirm that the observed effect is not due to heat. Finally, tests will be carried on on a few samples of 7, 14 and 60 days of age. Their analysis will show how sonication affects the kinetic evolution of cement paste's mechanical properties.

Nevertheless, results obtained so far raise serious doubts as to the relevance of the use of ultrasound in the cement industry. And on a more fundamental point of view, they show how complex and fascinating an out-of-equilibrium material like cement can be, since its long-term properties as a hardened paste can be dramatically affected by a modification of its very early history as a liquid gel.

References

[1] Eshmaiel Ganjian, Ahmad Ehsani, Timothy J. Mason, and Mark Tyrer. Application of power ultrasound to cementitious materials: Advances, issues and perspectives. *Materials & Design*, 160:503–513, December 2018.

[2] Andrew J. Allen, Jeffrey J. Thomas, and Hamlin M. Jennings. Composition and density of nanoscale calcium–silicate–hydrate in cement. *Nature Materials*, 6(4):311–316, April 2007.

[3] Katerina Ioannidou. Mesoscale Structure and Mechanics of C-S-H. In Wanda Andreoni and Sidney Yip, editors, *Handbook of Materials Modeling: Applications: Current and Emerging Materials*, pages 1–15. Springer International Publishing, Cham, 2018.

[4] Georgios Constantinides and Franz-Josef Ulm. The effect of two types of C-S-H on the elasticity of cement-based materials: Results from nanoindentation and micromechanical modeling. *Cement and Concrete Research*, 34(1):67–80, January 2004.

[5] Katerina Ioannidou, Matej Kanduč, Lunna Li, Daan Frenkel, Jure Dobnikar, and Emanuela Del Gado. The crucial effect of early-stage gelation on the mechanical properties of cement hydrates. *Nature Communications*, 7:12106, July 2016.

[6] Simone Peters. *The influence of power ultrasound on setting and strength development of cement suspensions*. PhD thesis, Fakultät Bauingenieurwesen der Bauhaus-Universität Weimar, 2017.

[7] W. C. Oliver and G. M. Pharr. Measurement of hardness and elastic modulus by instrumented indentation: Advances in understanding and refinements to methodology. *Journal of Materials Research*, 19(1):3–20, January 2004.

[8] Matthieu Vandamme and Franz-Josef Ulm. Nanogranular origin of concrete creep. *Proceedings of the National Academy of Sciences*, 106(26):10552–10557, June 2009.

[9] Ange-Therese Akono, Pedro Miguel Reis, and Franz-Josef Ulm. Scratching as a Fracture Process: From Butter to Steel. *Physical review letters*, 106:204302, May 2011.

[10] Ange-Therese Akono, Nicholas X. Randall, and Franz-Josef Ulm. Experimental determination of the fracture toughness via microscratch tests: Application to polymers, ceramics, and metals. *Journal of Materials Research*, 27(2):485–493, January 2012.

[11] Pooyan Kabir, Franz-Josef Ulm, and Ange-Therese Akono. Rate-independent fracture toughness of gray and black kerogen-rich shales. *Acta Geotechnica*, 12(6):1207–1227, December 2017.

[12] Franz-Josef Ulm, Matthieu Vandamme, Chris Bobko, Jose Alberto Ortega, Kuangshin Tai, and Christine Ortiz. Statistical Indentation Techniques for Hydrated Nanocomposites: Concrete, Bone, and Shale. *Journal of the American Ceramic Society*, 90(9):2677–2692, 2007.